# Flight control and collision avoidance of three UAVs following each other

Zarina A. KUTPANOVA[1], Hakan TEMELTAS[2], Serik A. KULMAMIROV[3]

*Corresponding author
*,[1]Department of System Analysis and Management,
L.N. Gumilyov Eurasian National University,
010008, 2 Satpayev Str., Nur-Sultan, Republic of Kazakhstan,
zarina.kutpanova@outlook.com
[2]Department of Control and Automation, Istanbul Technical University,
34469, Maslak, Istanbul, Republic of Turkey
[3]Department of Artificial Intelligence and Big Data,
Al-Farabi Kazakh National University,
050040, 71 al-Farabi Ave., Almaty, Republic of Kazakhstan

DOI: 10.13111/2066-8201.2022.14.4.7

*Received: 22 August 2022/ Accepted: 03 November 2022/ Published: December 2022*


***Abstract:*** *An unmanned aerial vehicle is a hardware and software complex with multi-purpose control. Unlike manned aviation, an unmanned aerial vehicle requires additional modules in its control system. These include the drone itself, the operator's workplace, software, data transmission lines and blocks necessary to fulfil the set flight objectives. The range of applications of unmanned aerial vehicles in the civil sector is not limited, but with the current state of the legal framework for the use of airspace, flight operations are somewhat difficult. The article formulates the main scientific position on the methodology of solving auxiliary tasks set in the work. The methodology specifies the main research stages, and it is a generalized methodological algorithm for the implementation of scientific research, which provides theoretical developments, field observations and simulation computer modelling. As a result of the study, it was found that the motion control systems of unmanned aerial vehicles are used for the process of their differentiation by the principle of complete external control, the advantages of which are considered in the work. For external control of divergence process of unmanned aerial vehicles, a method is considered for assessing the situation of convergence of unmanned aerial vehicles and choosing the manoeuvre of their difference using the area of dangerous courses, unmanned aerial vehicles approach, and it is possible to take into account the inertia of unmanned aerial vehicles when turning and the presence of navigational hazards that are in the manoeuvring area.*

***Key Words***: *aircraft, movement, speed, manoeuvre, distance of closest approach, the process of divergence*

## 1. INTRODUCTION

During the control of the aircraft movement, aerodynamic forces and moments arise [1]. The angles of deviation in pitch, yaw, roll and thrust of the engine are used as regulatory factors that allow influencing the aircraft to control its movement. An unmanned aerial vehicle (UAV) as a control object is a complex dynamic system due to the presence of a large number of interconnected parameters and complex cross-interactions between them [2]. Complex motion is often divided into the simplest types: angular motion and the movement of the centre of mass, longitudinal and lateral motion [3]. The controls that create control actions can be divided into two groups: longitudinal controls that provide movement in the longitudinal plane; lateral motion controls that provide the required nature of changes in the angles of roll, slip and yaw [4].

The engine control channel regulates thrust in accordance with the specified flight program [5, 6]. Stable flight control is impossible without creating an acceptable quality automatic control system [7, 8]. For example, the aircraft control system serves to ensure flight along a given trajectory by creating the necessary aerodynamic forces and moments on the wing and fins [9]. Three types of control systems are possible – manual, semi-automatic and automatic [10]. In the manual control system, the pilot operator, assessing the situation, ensures the generation of control impulses and, using command levers through the control panels, deflects the steering surfaces, holding them in the desired position [11]. In a semi-automatic system, the pilot operator control signals are transformed and amplified by various automata and amplifiers, providing optimal stability and controllability characteristics of the aircraft [12, 13]. Automatic systems provide full automation of individual flight stages, freeing the pilot operator from direct involvement in the control of the aircraft [14].

In the process of adjusting the control by the angles or height of the aircraft flight in the automatic system, the desired values of angles or height are received at the input of the controller, and the output variables of the controller will deflect the angles of the ailerons along the pitch, roll and yaw channels [15, 16]. The task of the synthesis of the aerobatic system is to select the structure and parameters of the control channels that provide a given quality of flight control, based on dynamic properties. Actuators are an integral part of automatic UAV motion control systems [17, 18]. The inclusion of mathematical models of these devices in the control object allows taking into account their dynamic and static properties [19]. Steering actuators are selected from the condition that their load characteristics provide the necessary dynamics of control processes. In other words, they are required to ensure that the steering body loaded with external forces or external moments moves at a given speed [20]. The purpose of the study is to ensure the implementation of the requirements for the control system: the choice of a transition process with minimal time, the absence of overshoot (aperiodic process). It is necessary that the control system provides the specified parameters of the transition process. The goal set in this paper requires the study of the following tasks:

– justification of the mathematical description of the control object (CO);
– building a simulation model;
– study of the dynamics of the model;
– implementation of the laws of management of the management object.

## 2. MATERIALS AND METHODS

It is necessary to find analytical expressions for the boundaries of the area of dangerous courses and UAV speeds, taking into account the ratio of their speeds, based on the condition of equality of the distance of UAV's closest approach and the maximum permissible approach distance. Since the distance of the closest approach of the UAV depends on the course of the first UAV and on the speed of the second UAV, which are the parameters of the divergence manoeuvre, and the maximum permissible distance of approach is a constant, the relationship between the course of the first UAV and the speed of the second UAV is derived from the obtained equality, which is the equation of the limits of the area of dangerous courses and UAV speeds.

The area obtained in this way is used to determine a safe joint divergence manoeuvre if the turn and braking time of the UAV is insignificant and can be neglected. In the case of a significant braking time of the second UAV, a procedure for the area development should be developed, and the development algorithm should differ from the previous one. To take into account the influence of the inertial braking characteristics of the second UAV on the possibility of divergence in the selected maximum permissible approach distance, it is necessary to use analytical expressions of the characteristics of the processes of active and passive braking.

The next stage of the work is the development of a method for accounting for the third UAV, which may interfere with the safe distinction of the first and second UAV. To solve the next stage, an analytical procedure should be developed to determine the distances of the closest approach of the third UAV with the first and second UAVs during their divergence. If these distances are greater than the maximum permissible approach distance, then a compatible manoeuvre selected using the area of dangerous values of the course of one UAV and the speed of the other is acceptable, since it ensures the safe divergence of all three UAVs. Then it is necessary to develop a way to visualize the developed area of dangerous values of the course and speed of the UAV and to form a verbal algorithm for determining the parameters of a safe manoeuvre of divergence at the selected point of the boundary of the developed area.

## 3. RESULTS AND DISCUSSIONS

To ensure the safety of the difference, the coordination of the UAV divergence manoeuvres is necessary, that is, the coordination of manoeuvres, which allows increasing the distance of the closest approach. With this type of control, each of the UAVs controls the current state of the approach situation and when a situational disturbance occurs, Bz interaction occurs between the UAVs, which transforms the programme section of relative motion with situational disturbance ($D_{min} < D_d$) into a relative trajectory without situational disturbance $\left(D_{miny} \geq D_d\right)$. The Bz interaction predicts the behaviour of UAVs in case of divergence and ensures the development of coordinated targeted strategies for each of the interacting UAVs. Therefore, the interaction of Bz can formally be written in this way:

$$G = Bz(F) \tag{1}$$

where $F = (D, \alpha, V_1, K_1, V_2, K_2)$ – is the vector of the convergence situation, $G = (G_1, G_2)$.

Thus, the interaction of the UAV Bz is the operator or the display of the parameters of the state of the approach situation in the set of parameters of the strategy difference G, and the interaction of Bz consists of two operators: *Crd* – coordination of manoeuvres and *Prm* – calculation of manoeuvre parameters.

The interaction of Bz, as a mechanism of coordination to achieve the common goal of preventing dangerous convergence, indicates the behaviour of each of the UAVs in the process of divergence, and a change in the situation is predicted, which is an extremely important factor affecting the safety of the difference. Thus, the process of differentiation is the process of compensating situational disturbance, that is, transferring the situation of convergence into a subset of safe states, according to the interaction mechanism Bz, and the strategy of difference G is the algorithm for implementing the process of divergence. The implementation of the Bz interaction is carried out using a binary coordination system or a $c_o$(Bz) coordinator, the input of which is a vector *F*, and the output is the address signals of the UAV $\beta_1$ and $\beta_2$ (Figure 1).

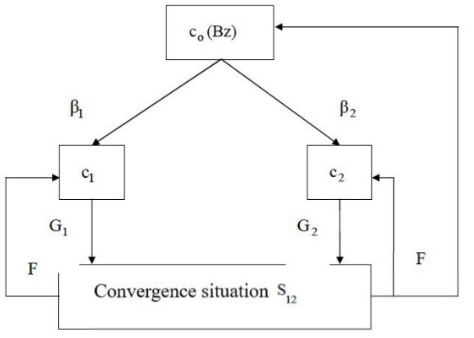


Figure 1. Independent control of the $S_{12}$ system

With the help of the address signal $\beta_i$ and the state vector *F*, each of the UAVS $c_i$ of the $S_{12}$ system selects a manoeuvre of divergence $G_i$ from the permissible subset of evasion courses, which is regulated by the coordinating signal $\gamma_i$. The $c_o$(BZ) binary coordination system is a means for describing the behaviour trend of a pair of interacting UAVs when a situational disturbance occurs in order to compensate for it. As a divergence manoeuvre, the manoeuvre of changing the course of the UAV is considered. First of all, the binary coordination system $c_o$(BZ) must satisfy Ashby's law of necessary diversity, according to which the variety of available difference strategies must correspond to the variety of possible situational perturbations. Otherwise, the $c_o$(BZ) system will not be able to compensate for situational disturbances, creating prerequisites for UAV collisions. This means that the system $c_o$(BZ) must have at its disposal the potential possibility of compensating situational disturbance in all cases at $\omega_1$.

In conditions of reduced visibility, UAV coordination is not provided for in the MPPSS-72 standard. The second type of control of the UAV divergence process is their complete control by an external UAV operator, who observes the state of the convergence process and, in the event of a situational disturbance, develops a common divergence strategy for both UAVs, translating a dangerous convergence into an unfulfilled state. This type of control can be both a workstation control system (WCS) and, crucially, an on-board information system with the same capabilities installed on each of the UAVs, which solves the problem of collective compensation of situational disturbance and implements the individual strategy obtained as a result of the solution. The UAV operator Ξobserves the state vector F of the situation S of $_{12}$ approaching UAVs and analyses the presence of a situational disturbance, at the appearance of which the operator chooses the optimal strategy ($G_1$, $G_2$). Manoeuvres $G_1$ and $G_2$, as shown in Figure 2, are addressed to the UAVs $c_1$ and $c_2$ that implement them.

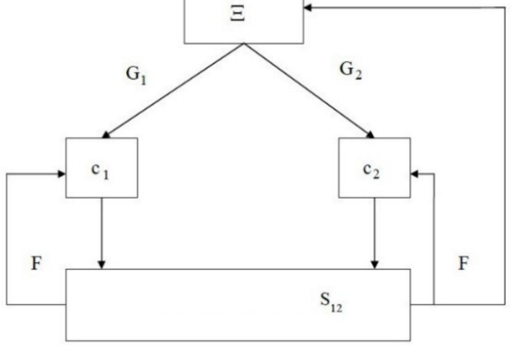


Figure 2. The principle of complete control of the $S_{12}$ system

The advantage of full control of the divergence process by the UAV operator by an external manager is the same interpretation of situational disturbance when choosing divergence manoeuvres $G_1$ and $G_2$. Compensation of situational disturbance ω is developed in the first phase of evasion strategy G. After the completion of the evasion section, the exit section to the program trajectory of movement is realised. Recently, methods of external control of the UAV divergence process have been suggested, in particular, the paper considers the method of developing the area of dangerous UAV courses and procedures for assessing the situation of convergence and choosing evasion courses with its help. Here is a brief outline of the essence of the method of developing a dangerous area of UAV courses and its application. Let's assume that at the initial moment of time, the mutual position of two UAVs that are dangerously approaching is characterised by the bearing $a_{ij}$ and the distance $D_{ij}$, and the mutual displacement is the relative course $K_{otij}$ and the speed $V_{otij}$. The distance of the closest approach min $D_{ij}$ of the UAV is less than the maximum permissible distance d, that is, min $D_{ij} < d_d$, and the UAVs are approaching dangerously. The WCS, which controls the flight of the UAV, needs to find the courses of the UAV $K_i$ and $K_j$, at which their distances of the closest approach will be greater than the maximum permissible distance $d_d$. For this purpose, we use the expression (1) for min $D_{ij}$ and get:

$$minD_{ij} = \Delta_{ij} D_{ij} \sin(\alpha_{ij} - K_{otij}) \geq d_d \tag{2}$$

The minimum approach distance min $D_{ij}$ can be increased by changing the relative course $K_{otij}$, that is, the courses of the UAV $K_i$ and $K_j$. Let's find the value of the UAV courses that ensure the fulfillment of the obtained condition, which can be represented as:

$$tgK_{otij} \leq tg\left[\alpha_{ij} - arc\sin\frac{d_d}{\Delta_{ij} D_{ij}}\right] \tag{3}$$

Enter the designation:

$$\gamma_{ij} = \alpha_{ij} - arc\sin\left(\frac{d_d}{\Delta_{ij} D_{ij}}\right) \tag{4}$$

and we take into account that according to:

$$tgK_{otij} = \frac{V_i \sin K_i - V_j \sin K_j}{V_i \cos K_i - V_j \cos K_j} \tag{5}$$

with this in mind, expression (23) takes the following form:

$$(\sin K_i \cos \gamma_{ij} - \cos K_i \sin K_{ij}) \leq \rho_{ij}(\sin K_j \cos \gamma_{ijj} - \cos K_j \sin \gamma_{ij}) \tag{6}$$

where:

$$\rho_{\text{шо}} = V_j / V_i \tag{7}$$

Corresponding equality:

$$(\sin K_1 \cos \gamma_{ij} - \cos K_i \sin \gamma_{ij}) = \rho_{ij}(\sin K_j \cos \gamma_{ij} - \cos K_j \sin \gamma_{ij}) \tag{8}$$

or:

$$\sin(K_i - \gamma_{ij}) = \rho_{ij}[\sin(K_j - \gamma_{ij})] \tag{9}$$

represents analytical expressions of the boundary of the dangerous area $S_{Dij}$, which limits the invalid value combinations of the pairs of corresponding courses $K_i$ and $K_j$.

The resulting equation has two solutions, that is, the following analytical dependencies are valid:

$$K_i - \gamma_{ij} = arc\sin\{\rho_{ij}[\sin(K_j - \gamma_{ij})]\} \tag{10}$$

$$K_i - \gamma_{ij} = \pi - arc\sin\{\rho_{ij}[\sin(K_j - \gamma_{ij})]\} \tag{11}$$

The first of the two solutions of the equation correspond to the situation of approaching UAVs, and the second corresponds to the situation of their removal. The danger of collision occurs when the UAV approaches, therefore, the equation of the boundaries of the dangerous areas of the courses $S_{Dij}$ is determined by the equation:

$$K_i = \gamma_{ij} + arc\sin\{\rho_{ij}[\sin(K_j - \gamma_{ij})]\} \tag{12}$$

This expression characterizes the boundary between the dangerous and permissible areas of the courses $K_i$ and $K_j$. Using the program, Figure 3 shows a graphical representation of the dangerous area $S_{Dij}$ of the courses $K_i$ and, in which min $D_{ij} < d_d$, for a situation of dangerous approach with parameters $\alpha = 75°$, $D = 3$ miles, $d_d = 1$ mile, $V_i = 15$ nodes, $V_j = 20$ nodes.

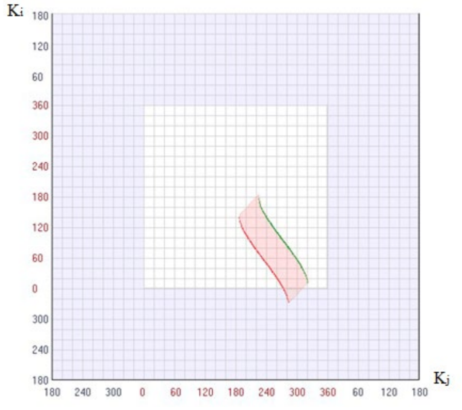


Figure 3. Dangerous area $S_{Dij}$ of courses $K_i$ and $K_j$ at $V_i < V_j$

If the UAV speeds are equal, that is $V_i = V_j$, it follows:

$$K_i - \gamma_{ij} = arc\sin\{[\sin(K_j - \gamma_{ij})]\} \tag{13}$$

$$K_i - \gamma_{ij} = \pi - arc\sin\{[\sin(K_j - \gamma_{ij})]\} \tag{14}$$

The convergence condition corresponds to the dependence, the graphical form of which is shown in Figure 4.

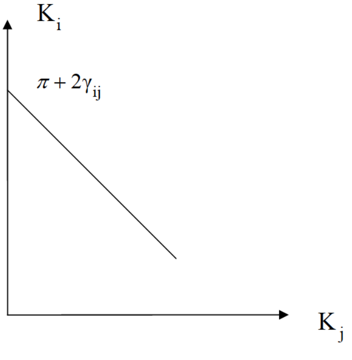


Figure 4. Dependence of the $K_i$ course from $K_j$

Figure 5 shows the danger area $S_{Dij}$ of courses $K_i$ and $K_j$ for the same situation, but with $V_i$ = 15 nodes, $V_j$ = 15 knots. Please note that when the UAV speeds are equal, the boundaries of the area of dangerous approaching courses $S_{Dij}$ are straight lines.

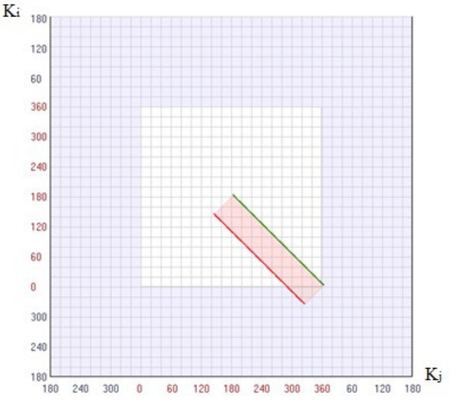


Figure 5. Dangerous area $S_{Dij}$ of courses $K_i$ and $K_j$ at $V_i = V_j$

If $V_i > V_j$, that is, $p_{ij} < 1$, then the dependence between the courses of the UAV $K_i$ and $K_j$ for the case of convergence is expressed as follows:

$$K_i = \gamma_{ij} + arc\,\sin\{\rho_{ij}[\sin(K_j - \gamma_{ij})]\} \tag{15}$$

Since $p_{ij} < 1$, the course $K_j$ takes all values from 0 to 2π. Figure 6 shows the danger area $S_{Dij}$ of courses $K_i$ and $K_j$ for $V_i$ = 20 nodes, $V_j$ = 15 knots.

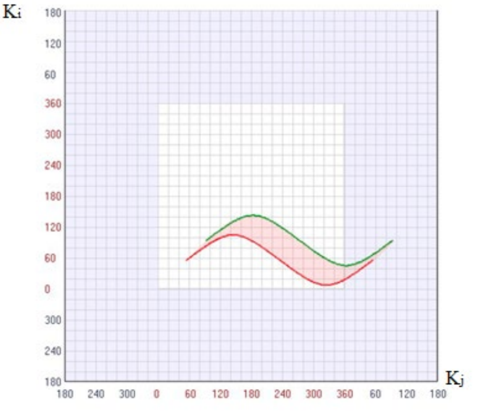


Figure 6. Dangerous area $S_{Dij}$ of courses $K_i$ and $K_j$ at $V_i > V_j$

The assessment of the danger of the approach situation is carried out by analysing the position of the point of the UAV's initial courses ($K_{ni}$, $K_{nj}$) in relation to the dangerous area $S_{Dij}$. If $(K_{ni}, K_{nj}) \in S_{Dij}$, then $minD_{ij} < d_d$ the situation of convergence is dangerous, otherwise there is no situational disturbance and there is no need to change the parameters of the movement of UAVs approaching. As an example, Figure 7 shows the danger area S $_{Dij}$ for the following parameters: $\alpha_{ij} = 90^o$, $D_{ij}$ = 3.0 miles, $d_d$ = 1.0 mile, $V_i$ = 15 nodes, $V_j$ = 20 nodes. For the initial courses $K_{ni} = 45^o$, and $K_{nj} = 315^o$, the starting point is located in the dangerous area of the courses (in Figure 7, the course $K_j$ is counted along the ordinate axis and displayed by a horizontal line, and the course $K_i$ is counted along the abscissa axis and displayed by a vertical line). For a given point, the distance of the closest approach is min $D_{ij}$ = 0.42 miles, so it is necessary to change the position of the point ($K_i$, $K_j$) by transferring its position from the dangerous area $S_{Dij}$. For this purpose, a point M is selected that belongs to the boundary of the region $S_{Dij}$ at the minimum distance from the starting point. The coordinates of this point are the values of the optimal UAV evasion courses. Figure 7 shows that the optimal values of the courses are $K_i = 63^o$, $K_j = 323^o$ – they are the coordinates of the point M, while $\Delta K_i = 18^o$ and $\Delta K_j = 8^o$. At the specified UAV courses, the distance of the closest approach min $D_{ij}$ = 1.01 miles, that is, equal to the maximum permissible distance.

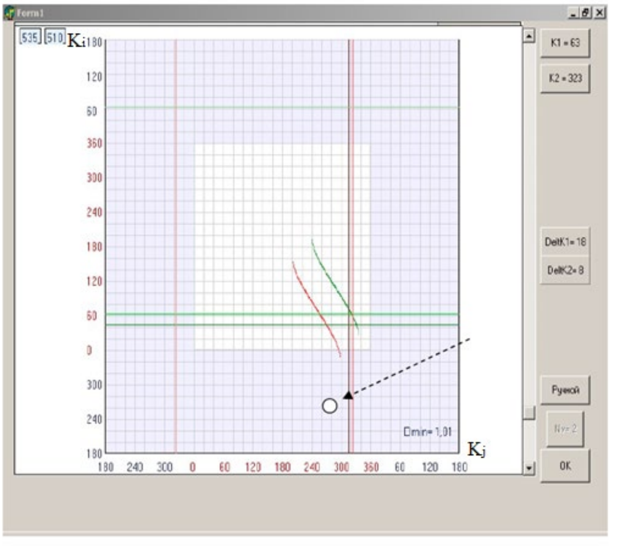


Figure 7. Determination of optimal values of courses $K_i$ and $K_j$

Taking into account the inertia of the UAV when turning and navigational obstacles in the development of the area of dangerous courses and the choice of optimal evasion courses are considered in the work, and the inertia of the UAV when turning is taken into account by a dynamic rotation model with a constant angular velocity at a given rudder angle. Navigational hazards are taken into account by a set of unacceptable evasion courses, which is set by a pair of boundary unacceptable courses for each UAV. Thus, having at your disposal the dangerous area $S_{Dij}$ of the courses of two UAVs, you can choose safe evasion courses that provide a discrepancy at a distance that is greater than the maximum permissible distance, while it is possible to take into account the inertia of the UAV and navigational obstacles.

In our work, it is shown that at the value of the difference between the courses of the UAV $\Delta K = 0$ and $\Delta K = 180$ , that is, when the UAV approaches on "countercourses" and parallel courses, the change in the speeds of the UAV does not affect the value of the relative course. Therefore, in such situations, the UAV divergence manoeuvre by changing speeds is impossible, that is, many safe divergence manoeuvres are empty. The paper also indicates that when the current UAV speeds are equal, the $(\Delta V = 0)$value of the relative course also does not change. Therefore, in the case of equality of the initial speeds with their identical change, the manoeuvre of divergence of the UAV by changing the speeds is also impossible.

It was shown above that the area of unacceptable speeds of a pair of UAVs has limits:

$$V_1^* = k^* V_2, V_{1^*} = k_* V_2 \tag{16}$$

where:

$$k^* = \frac{\sin(K_2 - \gamma^*)}{\sin(K_1 - \gamma^*)} \; and \; k_* = \frac{\sin(K_2 - \gamma_*)}{\sin(K_1 - \gamma_*)}. \tag{17}$$

Obviously, the existence of many safe manoeuvres of difference takes place under the condition:

$$\infty > k^* > 0, \infty > k_* > 0 \text{ and } k^* > k_* \quad (18)$$

Otherwise, the plural of safe divergence maneuvers is empty. The existing area of dangerous speeds has the form shown in Figure 8. In this example, the parameters of the convergence situation have the following values:

$$\alpha_0 = 45°, D_0 3 \text{ miles}, D_d = 1 \text{ mile}, K_1 = 90°, K_2 = 180° \quad (19)$$

At initial speeds $V_1$ = 18 knots and $V_2$ = 21 knots, the distance of the shortest approach is $D_{min}$ = 0.23 miles.

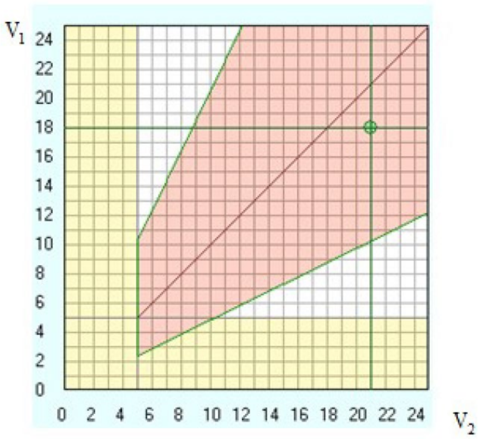


Figure 8. The area of dangerous UAV speeds

The above conditions are also valid for taking into account the inertial characteristics of the UAV when choosing a safe manoeuvre. In this case, to select their divergence rates, it has to be done as follows. A pair of safe speeds $V_{1y}$ and $V_{2y}$ of the area of dangerous speeds is determined. Due to the inertia of the UAV, the necessary speed differences $V_{1y}$ and $V_{2y}$ are achieved over time intervals in accordance with $\tau_{1y}$and $\tau_{2y}$, which are not equal to each other. Through this the total duration of the transition process $t_p$ from the beginning of the UAV velocity change in the selected stable values $V_{1y}$ and $V_{2y}$ is equal to the larger of the intervals

$$\tau_{1y} \text{ and } \tau_{2y}\left(t_p = max\left[\tau_{1y}, \tau_{2y}\right]\right) \quad (20)$$

This work is devoted to the second type of optimal divergence manoeuvre by reducing the speed, the feature of which is a fixed value of the moment of the beginning of the braking of the UAV, equal to the zero moments of time $t_n$ = 0. The divergence manoeuvre is optimized according to the parameters $V_{1y}$ and $V_{2y}$, which differ minimally from the initial values of the corresponding velocities $V_1$, $V_2$ and ensure equality $D_{min}$ ($V_{1y}$, $V_{2y}$) = $D_d$ until the end of the transition process coinciding with the time of the closest approach.

To select the optimal manoeuvre of the second type, a programme has been developed that calculates the distance of the closest approach based on the entered values of the evasion speeds $V_{1y}$ and $V_{2y}$, taking into account the selected braking modes, and allows you to determine the optimal values of the UAV evasion speeds.

As an example, the situation of a dangerous approach of a UAV with speeds of $V_1$ = 17 knots and $V_2$ = 22 knots is considered. As shown in Figure 9, the convergence situation is dangerous because the initial velocity point ($V_1$, $V_2$) is in the region of dangerous velocities.

Active braking is selected for the divergence manoeuvre of the first and second UAVs. The choice of the evasion speed is carried out interactively, and the predicted value of the distance of the closest approach is indicated. First, the evasion speed $V_{1y}$ = 14.5 knots was introduced for the first UAV. Then the second UAV is selected, and the input of the evasion speed is completed when the distance of the closest approach reaches the maximum permissible distance (0.99 miles), as shown in Figure 9. At the same time, the speed of the second UAV is $V_{2y}$ = 6.5 knots. The point corresponding to the selected evasion speeds $V_{1y}$ = 14.5 knots and $V_{2y}$ = 6.5 knots is located near the boundary of the dangerous speeds area, and the evasion speeds are shown by dots on the UAV braking curves displayed on the right side of the monitor screen.

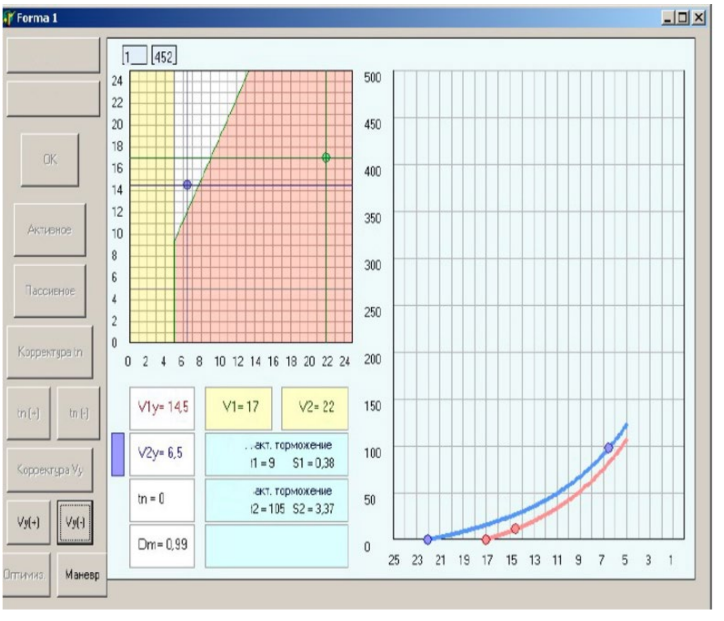


Figure 9. Selection of optimal UAV divergence speeds

Thus, with both types of optimal UAV divergence manoeuvres, the optimality criterion is the loss of the UAV's running time to perform the divergence manoeuvre, which must be minimised. This is expressed as follows. From the expression (1) for min *D* we get:

$$K_{ot} = \alpha \mp arc\sin\left(\frac{d_d}{D}\right) \tag{21}$$

therefore, equality is fair:

$$tgK_{ot} = tg\left[\alpha \pm arc\sin\left(\frac{d_d}{D}\right)\right] \tag{22}$$

Denoting it:

$$\gamma^{(1,2)} = \alpha \mp arc\sin\left(\frac{d_d}{D}\right) \tag{23}$$

therefore:

$$tgK_{ot} = tg\gamma^{(1,2)} \tag{24}$$

Taking into account:

$$tgK_{ot} = \frac{V_1 \sin K_1 - V_2 \sin K_2}{V_1 \cos K_1 - V_2 \cos K_2} \tag{25}$$

we will get:

$$\frac{V_1 \sin K_1 - V_2 \sin K_2}{V_1 \cos K_1 - V_2 \cos K_2} = \frac{\sin \gamma^{(1,2)}}{\cos \gamma^{(1,2)}} \tag{26}$$

therefore, we write down the relationship between the course of one UAV $K_1$ and the speed of another UAV $V_2$, which satisfy the condition min $D = d_d$. Expression (74) takes the following form:

$$\sin K_1 \cos \gamma^{(1,2)} - \cos K_1 \sin \gamma^{(1,2)} = \frac{V_2}{V_1}\left(\sin K_2 \cos \gamma^{(1,2)} - \cos K_2 \sin \gamma^{(1,2)}\right) \tag{27}$$

or:

$$\sin\left(K_1 - \gamma^{(1,2)}\right) = \frac{\sin\left(K_2 - \gamma^{(1,2)}\right)}{V_1} V_2 \tag{28}$$

If denote:

$$\mu^{(1,2)} = \frac{\sin\left(K_2 - \gamma^{(1,2)}\right)}{V_1} \tag{29}$$

that:

$$V_2^{(1,2)} = \frac{\sin\left(K_1 - \gamma^{(1,2)}\right)}{\mu^{(1,2)}} \tag{30}$$

So, there are two limits on which the equality min $D = d_d$ is achieved:

$$V_2^{(1)} = \frac{\sin\left(K_1 - \gamma^{(1)}\right)}{\mu^{(1)}} = \frac{V_1}{\sin\left[K_2 - \left(\alpha + arc\sin\frac{d_d}{D}\right)\right]} \sin\left[K_1 - \left(\alpha - arc\sin\frac{d_d D}{D}\right)\right] \tag{31}$$

$$V_2^{(2)} = \frac{\sin\left(K_1 - \gamma^{(2)}\right)}{\mu^{(2)}} = \frac{V_1}{\sin\left[K_2 - \left(\alpha - arc\sin\frac{d_d}{D}\right)\right]} \sin\left[K_1 - \left(\alpha + arc\sin\frac{d_d D}{D}\right)\right] \tag{32}$$

Since we are considering a change in speed by braking, the speed values $V_2^{(1,2)}$ must satisfy the condition $V_{2n} > V_2^{(1,2)} \geq 0$ where: $V_{2n}$ is the initial speed of the UAV, which changes its speed with a difference. Let's consider which values of the course $K_1$ correspond to the limit values 0 and $V_{2n}$ of the speed $V_2^{(1,2)}$. First of all, we note that the boundaries cannot be defined for a situation where:

$$K_2 = \alpha \pm arc\sin\frac{d_d}{D} \tag{33}$$

Obviously, from the boundary equations (33):

$$K_1\left(V_2^{(1,2)}(0) = \alpha \mp arc\sin\frac{d_d}{D} = \gamma^{(1,2)}\right) \tag{34}$$

To determine the second value:

$$K_1\left(V_2^{(1,2)}=V_{2n}\right) \tag{34'}$$

consider the equation:

$$V_2^{(1,2)}=\frac{\sin\left(K_1-\gamma^{(1,2)}\right)}{\mu^{(1,2)}} \tag{35}$$

and substitute $V_2^{(1,2)}=V_{2n}$:

$$V_{2n}=\frac{\sin\left(K_1-\gamma^{(1,2)}\right)}{\mu^{(1,2)}} \tag{36}$$

where from:

$$\sin\left(K_1-\gamma^{(1,2)}\right)=\frac{V_{2n}}{V_1}\sin\left(K_2-\gamma^{(1,2)}\right) \tag{37}$$

therefore:

$$K_1=\gamma^{(1,2)}+arc\sin\left[\frac{V_{2n}}{V_1}\sin\left(K_2-\gamma1^{(1,2)}\right)\right] \tag{38}$$

or:

$$K_1\left(V_2^{(1,2)}=V_{2n}\right)=\gamma^{(1,2)}+arc\sin\left[\frac{V_{2n}}{V_1}\sin\left(K_2-\gamma^{(1,2)}\right)\right] \tag{39}$$

In the case of $V_1 > V_{2n}$, there are values:

$$K_1\left(V_2^{(1,2)}=V_{2n}\right) \tag{40}$$

for both limits, and if $V_1 < V_{2n}$, then it is necessary to take into account the ratio between the magnitude $\gamma^{(1,2)}$ and the extreme relative rates $K_{otmax}$ and $K_{otmin}$.
Let's consider the case when $V_1>V_{2n}$ and find the limiting values of the course of the first UAV:

$$K_1\left(V_2^{(1)}=0\right)=\alpha-arc\sin\frac{d_d}{D}=\gamma^{(1)} \tag{41}$$

$$K_1\left(V_2^{(2)}=0\right)=\alpha+arc\sin\frac{d_d}{D}=\gamma^{(2)} \tag{42}$$

$$K_1\left(V_2^{(1)}=V_{2n}=\gamma^{(1)}+arc\sin\left[\frac{V_{2n}}{V_1}\sin\left(K_2-\gamma^{(1)}\right)\right]\right) \tag{43}$$

$$K_1\left(V_2^{(2)}=V_{2n}=\gamma^{(2)}+arc\sin\left[\frac{V_{2n}}{V_1}\sin\left(K_2-\gamma^{(2)}\right)\right]\right) \tag{44}$$

Let 's introduce the designation:

$$K_{1min}^{(1)}=K_1\left(V_2^{(1)}=0\right), K_{1min}^{(2)}=K_1\left(V_2^{(2)}=0\right) \tag{45}$$

$$K_{1min}^{(1)}=K_1\left(V_2^{(1)}=0\right), K_{1min}^{(2)}=K_1\left(V_2^{(2)}=0\right) \tag{46}$$

Taking into account the accepted designations:

$$K_{1min}^{(1)}=\alpha-arc\sin\frac{d_d}{D}=\gamma^{(1)} \tag{47}$$

$$K_{1min}^{(2)}=\alpha+arc\sin\frac{d_d}{D}=\gamma^{(2)} \tag{48}$$

$$K_{1max}^{(1)} = \gamma^{(1)} + arc\sin\left[\frac{V_{2n}}{V_1}\sin\left(K_2 - \gamma^{(1)}\right)\right] \tag{49}$$

$$K_{1max}^{(2)} = \gamma^{(2)} + arc\sin\left[\frac{V_{2n}}{V_1}\sin\left(K_2 - \gamma^{(2)}\right)\right] \tag{50}$$

We draw the reader's attention to the fact that the change in the speed of the second UAV $V_2$ in the section $V_2 \in (0, V_{2n})$ for the first limit occurs on the course section $K_1 \in \left(K_{1min}^{(1)}, K_{1max}^{(1)}\right)$, that is, on the interval:

$$\Delta K_1^{(1)} = K_{1max}^{(1)} - K_{1min}^{(1)} \tag{51}$$

or taking into account the expressions received:

$$\Delta K_1^{(1)} = arc\sin\left[\frac{V_{2n}}{V_1}\sin\left(K_2 - \gamma^{(1)}\right)\right] \tag{52}$$

Similarly, for the second limit: $K_1 \in \left(K_{1min}^{(2)}, K_{1max}^{(2)}\right)$:

$$\Delta K_1^{(2)} = arc\sin\left[\frac{V_{2n}}{V_1}\sin\left(K_2 - \gamma^{(2)}\right)\right] \tag{53}$$

In turn, the intervals $\Delta K_1^{(1)}$ and are $\Delta K_1^{(2)}$ smaller $\pi/2$, so at these intervals, the value of the velocity $V_2$ for both limits increase monotonically. Taking into account the results obtained, the area of $\Omega_{KV}$ dangerous parameters of the course of one UAV and the speed of the second UAV, bounded by the first $G_{1KV}$ and the second $G_{2KV}$ limits for the case $V_1 > V_{2n}$ and looks as shown in Figure 10. Thus, if the point with the initial parameters of the UAV motion $M_n$ ($K_{n1}$, $V_{2n}$) is located between the first $G_{1KV}$ and the second $G_{2KV}$ limits, that is $(K_{n1}, V_{2n}) \in \Omega_{KV}$, then the inequality min $D(K_{n1}, V_{2n})$ takes place $< d_d$, and the approach of the UAV is dangerous. In this case, you must select options evasion UAV $K_{1y}$ and $V_{2y}$, so that the corresponding point $M_y$ ($K_{1y}$, $V_{2y}$) was closest to the point of $M_n$ ($K_{n1}$, $V_{2n}$) of scope and the distance between the points $M_n$ and $M_y$ was minimal, as shown in Figure 10.

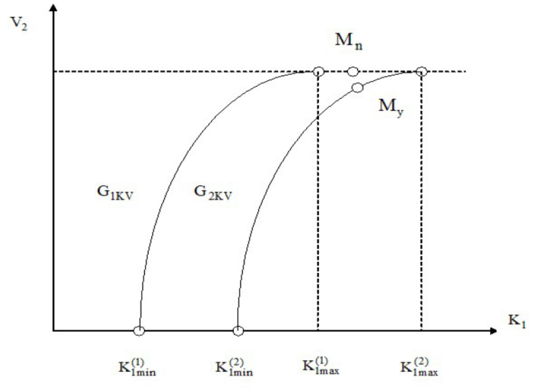


Figure 10. The area of $\Omega_{KV}$ dangerous parameters of the UAV

To calculate the evasion rate of the second UAV, which provides the distance of the closest approach equal to the maximum permissible approach distance for the selected evasion course of the first UAV, analytical expressions should be used for the duration of transients, the distance S travelled during this time and the dependence of the UAV speed on time in cases of active and passive braking. To do this, we will use the results of the work that enables us to obtain dependencies for active braking:

$$\tau_a = \frac{m}{\mu V_{yp}}\left[arctg\frac{V_0}{V_{yp}} - \frac{V_y}{V_{yp}}\right] \tag{54}$$

$$S_a = \frac{m}{2\mu}ln\left|\frac{V_0^2 + V_{yp}^2}{V_y^2 + V_{yp}^2}\right| \tag{55}$$

$$V_a = V_{yp}tg\left(arctg\frac{V_0}{V_{yp}} - \frac{\mu V_{yp}}{m}t\right) \tag{56}$$

Similarly, for passive braking mode:

$$\tau_p = \frac{m}{\mu}\left(\frac{1}{V_y} - \frac{1}{V_0}\right) \tag{57}$$

$$\tau_p = \frac{m}{\mu}\left(\frac{1}{V_y} - \frac{1}{V_0}\right) \tag{58}$$

$$S_P = \frac{m}{2\mu}ln\left|\frac{V_0^2}{V_y^2}\right| \tag{59}$$

Previously, a procedure was obtained for calculating the boundaries of the region $\Omega_{KV}$ in the case of the advantage of the speed of the first UAV ($V_1 > V_{2n}$). If the speed of the second UAV exceeds the speed of the first one, which manoeuvres a change of course, that is, $V_1<V_{2n}$, we get the equality:

$$K_1 = \gamma^{(1,2)} + arc\sin\left[\frac{V_{2n}}{V_1}\sin\left(K_2 - \gamma^{(1,2)}\right)\right] \tag{60}$$

the analysis of which shows that the boundary of the region $\Omega_{KV}$ exists for the velocities of the second UAV when the expression under the arcsin function:

$$\left|\frac{V_{2n}}{V_1}\sin\left(K_2 - \gamma^{(1,2)}\right)\right| \leq 1 \tag{61}$$

Therefore, the maximum value of the course of the first UAV $K_{1\max}$ of the boundary of the region is $\Omega_{KV}$ achieved at a speed of:

$$V_{2m} = \frac{V_1}{\sin(K_2 - \gamma^{(1,2)})} \tag{62}$$

and is equal to:

$$K_{1max} = \gamma^{(1,2)} \mp arc\sin(1) = \gamma^{(1,2)} \mp \frac{\pi}{2} \tag{63}$$

So:

$$K_{1max}^{(1,2)} = \gamma^{(1)} - \frac{\pi}{2}, K_{1max}^{(2)} = \gamma^{(2)} + \frac{\pi}{2} \tag{64}$$

Thus, for $V_1 < V_{2n}$, the boundaries of the area $\Omega_{KV}$ exist for:

$$K_1 \in \left[\gamma^{(1,2)} - \frac{\pi}{2}, \gamma^{(1,2)} + \frac{\pi}{2}\right] \text{ и } V_2 \in \left[0, \frac{V_1}{\sin(K_2 - \gamma^{(1,2)})}\right] \tag{65}$$

For the development of the area $\Omega_{KV}$ and its graphical display, a computer programme was developed that takes into account the ratio of the initial speeds of the UAV $V_1$ and $V_{2n}$. In the case of $V_1 > V_{2n}$, there are values:

$$K_1\left(V_2^{(1,2)} = V_{2n}\right) \tag{66}$$

for both limits, and the area of $\Omega_{KV}$ dangerous parameters of the course of one UAV.

The scientific result of solving the second auxiliary task was the methods of developing dangerous areas of UAV movement at the distance of the closest approach.

## 4. CONCLUSIONS

The article presents the essence of the principle of developing the area of dangerous parameters of the course of one unmanned aerial vehicle and the speed of the second unmanned aerial vehicle, as well as its application for choosing a safe divergence manoeuvre. The concept of situational disturbance that occurs in the case of a dangerous approach of unmanned aerial vehicles and an assessment of its level of danger is given; it is shown that when several unmanned aerial vehicles approach, a situational disturbance matrix is used. An analysis of the types of control of the divergence process of unmanned aerial vehicles in a dangerous approach is carried out. It is shown that the classical type of control of the collision process is locally independent control, which involves the use of a binary coordination system, which is currently implemented in the International Regulations for Preventing Collisions at Sea. The motion control systems of unmanned aerial vehicles are used for the process of their differentiation by the principle of complete external control.

For the external control of the unmanned aerial vehicles divergence process, a method of assessing the convergence situation of a pair of unmanned aerial vehicles and choosing their divergence manoeuvre using the hazardous path area is considered. Unmanned aerial vehicles are approaching, and the inertia of unmanned aerial vehicles when turning and the presence of navigational hazards that are in the manoeuvring area may be considered.

## REFERENCES

[1] G. S. Woo, D. Truong, W. Choi, Visual detection of small unmanned aircraft system: Modeling the limits of human pilots, *Journal of Intelligent and Robotic Systems*, **99**, 933-947, 2020.

[2] L. R. Sahawneh, J. K. Wikle, A. K. Roberts, J. C. Spencer, T. W. McLain, K. F. Warnick, R. W. Beard, Ground-based sense-and-avoid system for small unmanned aircraft, *Journal of Aerospace Information Systems*, **15**(8), 501-507 2018.

[3] L. R. Sahawneh, J. Mackie, J. Spencer, R. W. Beard, K. F. Warnick, Airborne radar-based collision detection and risk estimation for small unmanned aircraft systems, *Journal of Aerospace Information Systems*, **12**(12), 756-766, 2015.

[4] B. Rattanagraikanakorn, D. I. Gransden, M. Schuurman, C. de Wagter, R. Happee, A. Sharpanskykh, H. A. P. Blom, Multibody system modelling of unmanned aircraft system collisions with the human head, *International Journal of Crashworthiness*, **25**(6), 689-707, 2020 a.

[5] P. J. Highland, J. Williams, M. Yazvec, A. Dideriksen, N. Corcoran, K. Woodruff, C. Thompson, L. Kirby, E. Chun, H. Kousheh, J. Stoltz, T. Schnell, Modelling of unmanned aircraft visibility for see-and-avoid operations, *Journal of Unmanned Vehicle Systems*, **8**(4), 265-284, 2020.

[6] D. O. Batrakov, M. S. Antyufeyeva, A. V. Antyufeyev, A. G. Batrakova, UWB signal processing during thin layers thickness assessment, *2016 IEEE Radar Methods and Systems Workshop, RMSW 2016 - Proceedings,* 36-39, 2016.

[7] C. Minwalla, P. Thomas, K. Ellis, R. Hornsey, S. Jennings, Range performance evaluation from the flight tests of a passive electro-optical aircraft detection sensor for unmanned aircraft systems, *Journal of Unmanned Vehicle Systems*, **4**(2), 96-114, 2016 a.

[8] C. Kang, C. A. Woolsey, Model-based path prediction for fixed-wing unmanned aircraft using pose estimates, *Aerospace Science and Technology*, **105**, Article number: 106030, 2020.

[9] R. E. Tompa, B. Wulfe, M. J. Kochenderfer, M. P. Owen, Horizontal maneuver coordination for aircraft collision-avoidance systems, *Journal of Aerospace Information Systems*, **15**(2), 92-106, 2018.

[10] A. Weinert, S. Campbell, A. Vela, D. Schuldt, J. Kurucar, Well-clear recommendation for small unmanned aircraft systems based on unmitigated collision risk, *Journal of Air Transportation*, **26**(3), 113-122, 2018.

[11] R. A. Clothier, B. P. Williams, N. L. Fulton, Structuring the safety case for unmanned aircraft system operations in non-segregated airspace, *Safety Science*, **79**, 213-228, 2015.

[12] C. Minwalla, D. Tulpan, N. Belacel, F. Famili, K. Ellis, Detection of airborne collision-course targets for sense and avoid on unmanned aircraft systems using machine vision techniques, *Unmanned Systems*, **4**(4), 255-272, 2016 b.

[13] K. Lee, D. Choi, D. Kim, Incorporation of potential fields and motion primitives for the collision avoidance of unmanned aircraft, *Applied Sciences*, **11**(7), Article number: 3103, 2021.

[14] Y. Fu, Y. Zhang, X. Yu, An advanced sense and collision avoidance strategy for unmanned aerial vehicles in landing phase, *IEEE Aerospace and Electronic Systems Magazine*, **31**(9), 40-52, 2016.

[15] I. Cherunova, S. Tashpulatov, S. Kolesnik, Automation of deformed fibrous materials thermal characteristics accounting process in garments production, *2018 International Russian Automation Conference, RusAutoCon 2018,* Article number: 8501795, 2018.

[16] T. L. Molloy, T. Perez, B. P. Williams, Optimal bearing-only-information strategy for unmanned aircraft collision avoidance, *Journal of Guidance, Control, and Dynamics*, **43**(10), 1822-1836, 2020.

[17] D. O. Batrakov, M. S. Antyufeyeva, A. V. Antyufeyev, A. G. Batrakova, Remote sensing of plane-layered media with losses using UWB signals, *2017 11th International Conference on Antenna Theory and Techniques, ICATT 2017,* 370-373, 2017.

[18] E. D'Amato, M. Mattei, I. Notaro, Distributed reactive model predictive control for collision avoidance of unmanned aerial vehicles in civil airspace, *Journal of Intelligent and Robotic Systems*, **97**, 185-203, 2020.

[19] B. Rattanagraikanakorn, M. Schuurman, D. I. Gransden, R. Happee, C. de Wagter, A. Sharpanskykh, H. A. P. Blom, *Modelling head injury due to unmanned aircraft systems collision: Crash dummy vs human body*, https://www.tandfonline.com/doi/full/10.1080/13588265.2020.1807687, 2020 b.

[20] R. R. Lutz, P. S. Frederick, P. M. Walsh, K. S. Wasson, N. L. Fenlason, Integration of unmanned aircraft systems into complex airspace environments, *Johns Hopkins APL Technical Digest*, **33**(4), 291-302, 2017.